



Reliability Evaluation of Next Generation Inverter

Cooperative Research and Development Final Report

CRADA Number: CRD-12-478

NREL Technical Contact: Paul Paret

**NREL is a national laboratory of the U.S. Department of Energy
Office of Energy Efficiency & Renewable Energy
Operated by the Alliance for Sustainable Energy, LLC**

This report is available at no cost from the National Renewable Energy Laboratory (NREL) at www.nrel.gov/publications.

CRADA Report
NREL/TP-5400-67271
October 2016

Contract No. DE-AC36-08GO28308

NOTICE

This report was prepared as an account of work sponsored by an agency of the United States government. Neither the United States government nor any agency thereof, nor any of their employees, makes any warranty, express or implied, or assumes any legal liability or responsibility for the accuracy, completeness, or usefulness of any information, apparatus, product, or process disclosed, or represents that its use would not infringe privately owned rights. Reference herein to any specific commercial product, process, or service by trade name, trademark, manufacturer, or otherwise does not necessarily constitute or imply its endorsement, recommendation, or favoring by the United States government or any agency thereof. The views and opinions of authors expressed herein do not necessarily state or reflect those of the United States government or any agency thereof.

This report is available at no cost from the National Renewable Energy Laboratory (NREL) at www.nrel.gov/publications.

Available electronically at SciTech Connect <http://www.osti.gov/scitech>

Available for a processing fee to U.S. Department of Energy and its contractors, in paper, from:

U.S. Department of Energy
Office of Scientific and Technical Information
P.O. Box 62
Oak Ridge, TN 37831-0062
OSTI <http://www.osti.gov>
Phone: 865.576.8401
Fax: 865.576.5728
Email: reports@osti.gov

Available for sale to the public, in paper, from:

U.S. Department of Commerce
National Technical Information Service
5301 Shawnee Road
Alexandria, VA 22312
NTIS <http://www.ntis.gov>
Phone: 800.553.6847 or 703.605.6000
Fax: 703.605.6900
Email: orders@ntis.gov

Cover Photos by Dennis Schroeder: (left to right) NREL 26173, NREL 18302, NREL 19758, NREL 29642, NREL 19795.

NREL prints on paper that contains recycled content.

Cooperative Research and Development Final Report

In accordance with Requirements set forth in Article XI. Reports and Abstracts A.(3), of the CRADA agreement, this document is the final CRADA report, including a list of Subject Inventions, to be forwarded to the Office of Science and Technical Information as part of the commitment to the public to demonstrate results of federally funded research.

Parties to the Agreement: General Motors, LLC

CRADA Number: CRD-12-478

CRADA Title: Reliability Evaluation of Next Generation Inverter

Joint Work Statement Funding Table Showing DOE Commitment:

Estimated Costs	NREL Shared Resources
TOTAL	\$0.00

Abstract of CRADA Work:

In the operational environment of a power module in an electric drivetrain, high heat loads induce thermomechanical fatigue on the bonded interface layers within the module resulting in defects and/or delamination. Under thermal cycling, these defects gradually get bigger and can lead to catastrophic failure of the entire power module. Hence, it is essential to design reliable power modules that can withstand thermal loads. The Next-generation Inverter, which is being developed by GM, aims to address the U.S. Department of Energy (DOE) Vehicle Technologies Office (VTO) Electric Drive Technologies (EDT) Program targets for cost, specific power, and power density. The power module is an important part of an inverter, and it is essential for it to be high-performance and reliable. The experimental characterization and predictive lifetime model development efforts at NREL played a crucial role in evaluating the reliability of power modules and in its time- and cost-effective design.

Summary of Research Results:

In this project, NREL conducted two rounds of reliability evaluations. Description of test procedures, experimental and modeling results, and predictive lifetime model development are outlined in the sections below.

First Round of Testing

GM provided six power modules to NREL to be used as test samples for accelerated testing. For testing purposes, we altered the samples to allow for a non-obstructive pathway for imaging. The objective of the first round of testing was to characterize the reliability of die-attach solder in the power module, and develop a predictive lifetime model.

Accelerated Tests –Procedure and Results

Each of the six power modules were subjected to a thermal cycling accelerated test. The thermal cycle profiles are listed in Table 1.

Table 1. Thermal Cycling Profiles

Profile	Temperature Range (°C)	Dwell (mins)
1	25 to 125	15
2	0 to 100	15
3	-25 to 75	15
4	25 to 125	75
5	0 to 100	75
6	-25 to 75	75

All six profiles had a temperature difference of 100°C and a ramp rate of 5°C/min, but the mean temperature and dwell time varied. Temperature cycling was done in the benchtop chambers shown in Fig. 1.



Fig. 1. Accelerated test chambers

Prior to accelerated testing, as well as after every 100 cycles of accelerated testing, we took scanning acoustic microscope (C-SAM) images of the die-attach layers of all power modules to monitor any crack initiation and propagation.

Visual analysis of these C-SAM images revealed that no crack initiation or any other defects occurred in this power module due to the thermal cycling tests, a result that held true for all other power modules. This led to the conclusion that under the selected thermal profiles, it would take much longer periods of time to obtain any cycles-to-failure data. In light of these observations, we suggested revising the thermal cycling profiles to more aggressive profiles to cause faster failures, and based on discussions with GM colleagues, the power modules were then subjected to a revised set of thermal cycling profiles, which are listed in Table 2.

Table 2. Revised Thermal Cycling Profiles

Profile	Temperature Range (°C)	Dwell (mins)	Ramp Rate (°C/min)
1	-40 to 150	15	5
2	-40 to 150	30	5
3	-40 to 150	15	25
4	-40 to 125	15	5
5	-55 to 150	15	5
6	-65 to 125	15	5

The revised set of profiles encompasses variations in dwell time, ramp rates, mean temperature, and temperature difference. However, even after 800 thermal cycles with the revised temperature profiles, C-SAM images of the die-attach layer did not show any signs of crack initiation.

Lack of any signs of crack initiation in the die-attach layers of these power modules, even after accelerated testing under more severe thermal cycling profiles led us to the hypothesis/conclusion that reliability of an interface material is evaluated more quickly by testing large-area attachments. Results from our Department of Energy-sponsored bonded interfaces reliability project also reinforced the validity of this hypothesis, which was conveyed to GM.

Second Round of Testing

Description of Test Samples

Since accelerated testing of the first round of samples did not produce any failure data, a predictive model of the die-attach solder material could not be formulated. A second round of testing was initiated on a different test sample with bonded interface of a larger cross-sectional attach area.

There were three different sample types and the same solder material was used in all samples. We received 14 samples of type 1, and 15 each of type 2 and type 3.

Accelerated Tests – Procedure and Results

We developed an accelerated test plan, similar to the revised thermal cycling profiles in the first round of testing, for the new test samples. The accelerated test profiles and sample count allocated to each test profile is listed in Table 3.

Table 3. Accelerated Test Plan for the Second Round Testing

Profile	Low Temperature (°C)	High Temperature (°C)	Dwell (mins)	Ramp Rate (°C/min)	Number of Samples		
					Type 1	Type 2	Type 3
Standard	-40	150	15	5	4	4	4
Long Dwell	-40	150	30	5	4	4	4
Shock	-40	150	15	25	3	3	3
Low Delta	-40	125	15	5	3	4	4

We scanned all the samples using C-SAM prior to accelerated testing and found very minimal voiding or defects in most of the type 1 and type 2 samples. Type 3 samples had a higher amount of initial voiding, which was calculated to be around 5%. We found no cracks in any of the samples before accelerated testing.

Accelerated testing was then initiated for all the samples under various temperature profiles and the initial plan was to scan the samples after every 100-cycle intervals. However, C-SAM images of type 3 samples revealed aggressive rates of failure after the first 100 cycles, mainly due to the higher coefficient of thermal expansion (CTE) mismatch between its baseplate and substrate. Hence, we decided to scan all the samples at every 50-cycle intervals to capture more accurate cycles-to-failure data. Failure, in this project, was considered as the number of cycles at which the average value of crack areas in all samples of a type under a given accelerated test propagated to more than 30% of the total interface attachment area. We used ImageJ, a public domain image-processing program, to estimate the crack percentage in each C-SAM image. ImageJ calculates the pixel value statistics of a selected area in an image - a technique we employed in estimating the area-percentage of cracks. Cracks would appear as a different shaded region as compared with the bonded area. Prior to analyzing a C-SAM image, we darkened the white lines - which are actually the etch patterns in the top-metallization - in order to ensure that only the crack areas were calculated.

As accelerated tests progressed, type 3 samples under all test profiles reached failure faster than type 1 and type 2 samples. Between type 1 and type 2 samples, there was not much difference in cycles-to-failure, but in general, type 2 samples reached failure slightly faster than type 1 samples.

Under the *standard* accelerated test profile, type 1 and type 2 samples failed at 950 and 750 cycles, respectively, whereas type 3 samples reached failure at 400 cycles. Also, type 1 and type 2 samples exhibited similar rates of crack propagation until failure. Fig. 2 shows the rate of crack propagation in these samples up to failure.

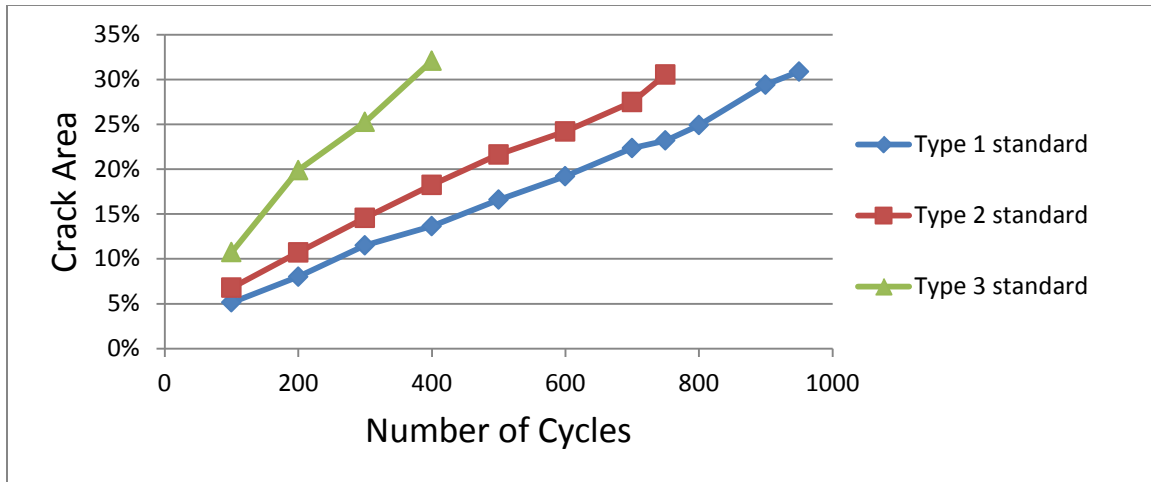


Fig. 2. Crack area versus number of cycles for type 1, type 2, and type 3 samples under the *standard* test profile.

Under the *long dwell* accelerated test profile, type 1 and type 2 samples failed at 700 and 650 cycles, respectively. It took just 250 cycles for type 3 samples to reach failure. In the *long dwell* test, samples are exposed to higher temperatures in a thermal cycle for longer period of time than in the *standard* test, thereby allowing for more creep to occur. This is the main reason why samples subjected to the *long dwell* profile exhibit faster rates of failure than *standard* samples. Fig. 3 shows the rate of crack propagation in these samples up to failure.

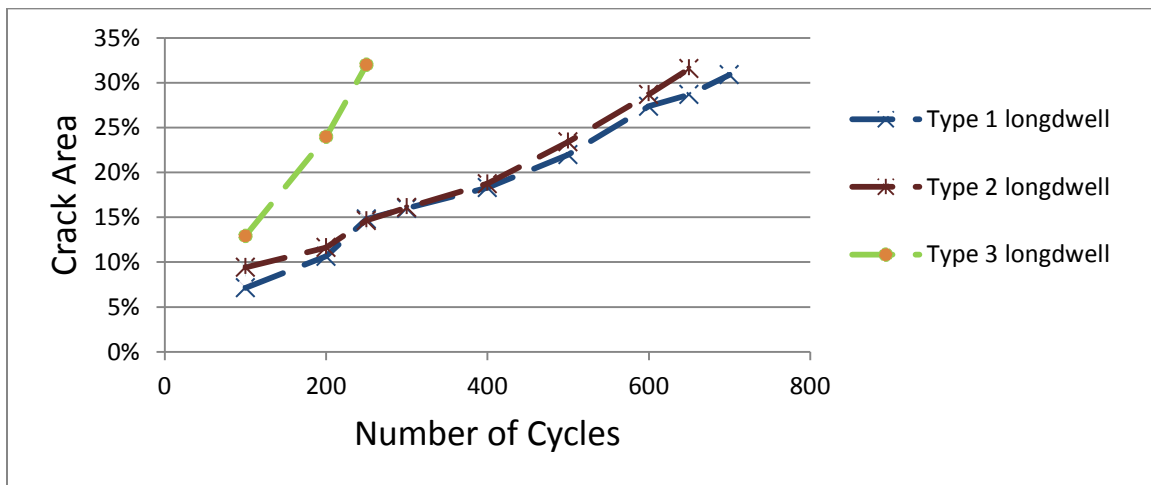


Fig. 3. Crack area versus number of cycles for type 1, type 2, and type 3 samples under the *long dwell* test profile.

Under the *shock* accelerated test profile, all sample types showed the same failure pattern as the *long dwell* samples - type 1, type 2, and type 3 samples failed at 750, 650, and 250 cycles, respectively. In the *shock* test, samples were exposed to rapid changes in temperature that resulted in a thermal gradient within the sample in addition to the CTE mismatch. As a result, a higher amount of stress was imparted on to the solder joint. Fig. 4 shows the rate of crack propagation in these samples up to failure.

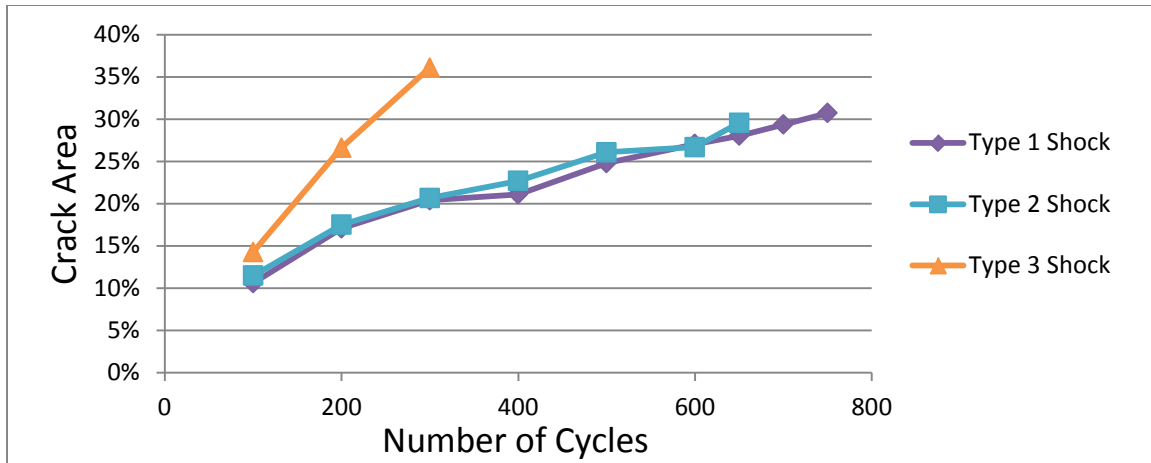


Fig. 4. Crack area versus number of cycles for type 1, type 2, and type 3 samples under the *shock* test profile.

The *low delta* accelerated test profile is the least aggressive of all test profiles due to the high-end temperature being lower than those in other test profiles. Samples subjected to this profile were expected to last longer than samples in other test profiles. Crack area in type 1 samples reached about 20 % in 900 cycles and started following a different growth rate thereafter. At 1,600 cycles, the calculated crack area was at around 25 % and we decided to halt further testing of these samples due to time constraints. We observed a similar variation in crack growth rate pattern in type 2 samples but the samples met the failure criterion at 1,500 cycles, as shown in Fig. 5. Type 3 samples failed at 750 cycles under the *low delta* test profile.

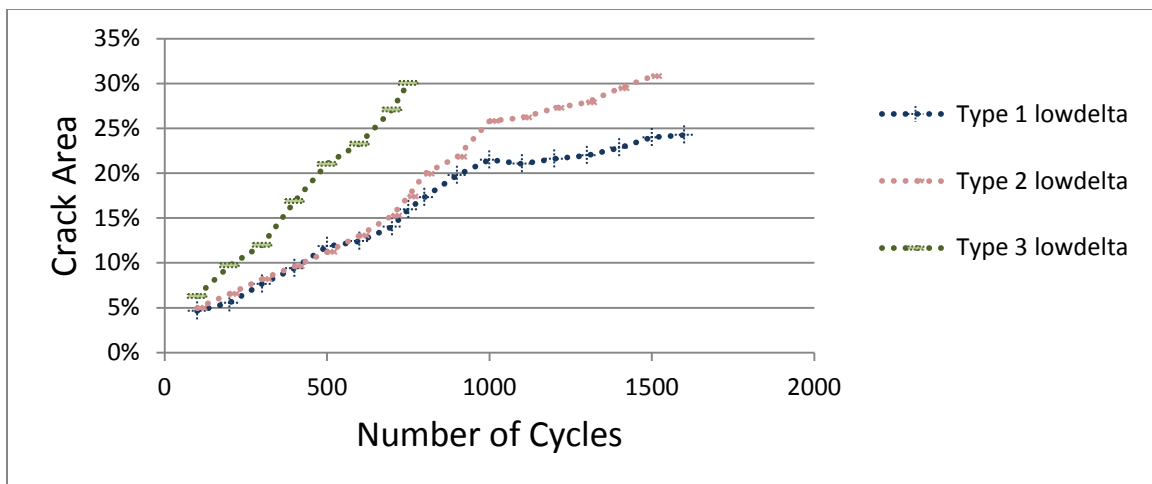


Fig. 5. Crack area versus number of cycles of type 1, type 2, and type 3 samples under the *low delta* test profile.

Thermomechanical Modeling

In addition to experimental accelerated testing of the second round of samples, we conducted a thermomechanical modeling study to obtain the required parameters to formulate a predictive lifetime model. In our Finite Element Method-based modeling study, we calculated strain energy density values of the solder joint in different sample types under various accelerated test profiles

as listed in Table 3. Strain energy density is defined as the time integral of the product of stresses and incremental strains in all six directions. We conducted the modeling study using ANSYS Mechanical, which is a widely used commercial software tool for structural analysis.

We obtained the required material properties of various components in the test sample from the literature. While linear elastic properties were adopted for baseplate and substrate materials, we selected the Anand model, a non-linear constitutive model, to simulate the viscoplastic nature of the solder layer. GM provided dimensions of the entire sample. A meshed geometry of the quarter-symmetric model built in ANSYS is shown in Fig. 6.

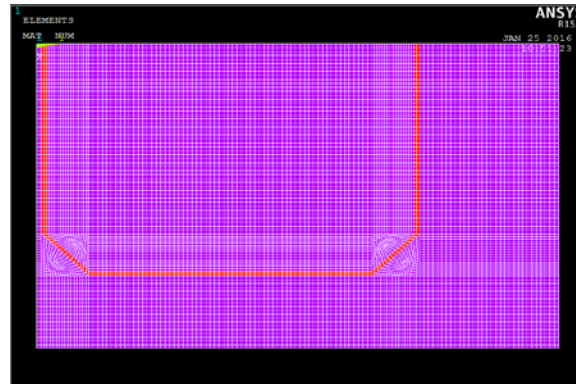


Fig. 6. Schematic of the test sample (on the left), quarter-symmetric model (on the right).

We ran a total of 12 simulations, which consisted of all the different combinations of sample type and accelerated test profiles, on Peregrine, NREL’s high-performance computing cluster. In post-processing of the results, the corner regions of the solder joint displayed higher values of strain energy density. Hence, we selected the chamfered area at the corner as the region of interest to calculate the volume-averaged strain energy density result. Fig. 7 shows a contour plot of strain energy density on the solder layer. The region of interest is highlighted by a red box.

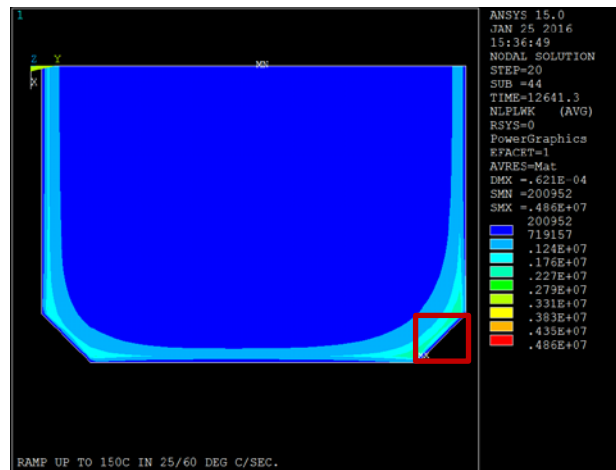


Fig. 7. Strain energy density contour plot.

Strain energy density values obtained from all 12 simulations are listed in Table 4 below.

Table 4. Strain Energy Density Results

Test Profile	Sample Type	Volume-averaged Strain Energy Density per Cycle (MPa)
Standard	Type 1	0.16
	Type 2	0.16
	Type 3	0.56
Long Dwell	Type 1	0.17
	Type 2	0.17
	Type 3	0.59
Shock	Type 1	0.18
	Type 2	0.18
	Type 3	0.63
Low Delta	Type 1	0.12
	Type 2	0.12
	Type 3	0.40

The only difference between type 1 and type 2 simulations were the slight variation in the ramp-down rate from its reflow temperature. This variation resulted in negligible differences between the residual stresses of the two sample types, which eventually got cancelled out in accelerated test loading. Type 3 samples under all test profiles had higher values of strain energy density, a reflection of the experimental results outlined in the previous section.

Predictive Lifetime Model

Predictive lifetime model of a solder material depends on the failure criterion, geometry of the sample, and the type of constitutive model employed in modeling. We developed an empirical correlation between the strain energy density per cycle and cycles-to-failure results of type 2 samples using a power-law model, which serves as the predictive lifetime model. Type 1 sample results could also have been chosen for developing the predictive lifetime model. The selection of type 2 sample results, for the development of the predictive lifetime model, in this project is purely arbitrary. However, since the poor initial bonding condition may have played a role in the short lifespan of type 3 samples, we realized that it is best not to use type 3 results to develop a lifetime model. Volume-averaged strain energy density per cycle was used as it captures both stress and strain information, and accurately represents the deformation behavior of solder joints. In Fig. 8, the red line denotes the results of type 2 samples, and the blue curve is the power-law fit - which is the predictive model.

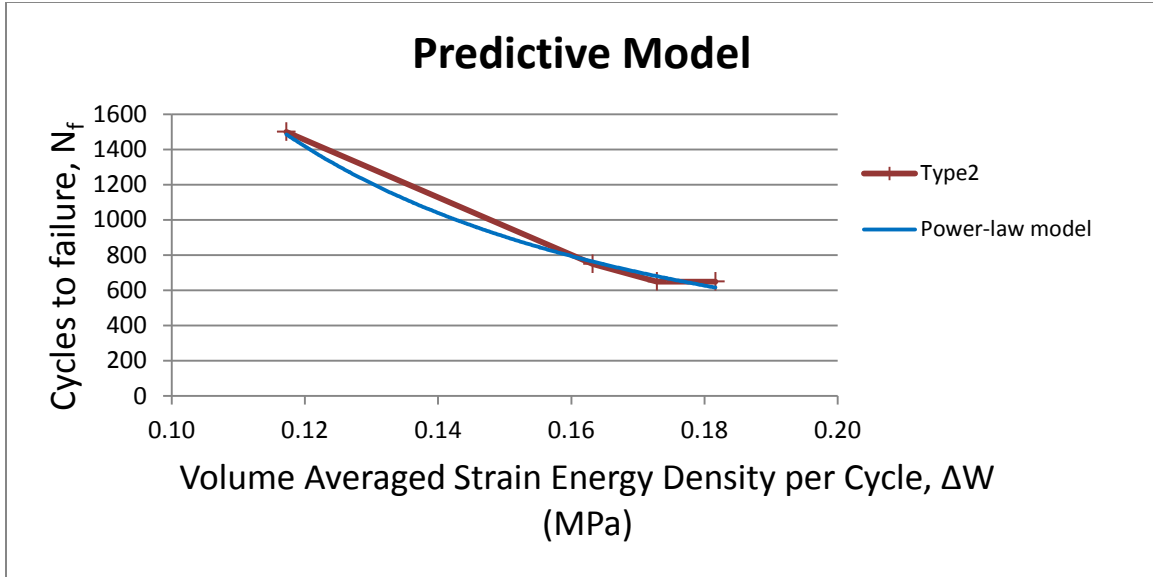


Fig. 8. Cycles-to-failure versus strain energy density plot

The predictive model from Fig. 8 is

$$N_f = 19.96 (\Delta W)^{-2.01}. \quad (1)$$

Here, N_f is the cycles-to-failure result obtained from experimental accelerated testing and ΔW is the volume-averaged strain energy density per cycle calculated from thermomechanical modeling. This predictive model can be used to estimate the reliability of the same solder joint with a similar geometry, and for the same failure mechanism and failure criterion that was observed and used in this work. We checked the accuracy of (1) by comparing the estimated cycles-to-failure of type 1 and type 3 samples with their actual cycles-to-failure obtained from experimental accelerated tests. The comparison is shown in Table 5.

Table 5. Comparison of Predictive Lifetime Model Results with Accelerated Test Results

Sample type	Test profile	Cycles-to-failure	Predicted cycles-to-failure from (1)
Type 1	Low Delta	N/A	1,487
	Standard	950	764
	Long Dwell	700	680
	Shock	750	616
Type 3	Low Delta	750	126
	Standard	400	63
	Long Dwell	250	58
	Shock	250	51

It can be seen in Table 5 that the developed predictive model is a few hundred cycles off in estimating the lifetime of type 3 sample. This shows that in addition to CTE mismatch, other factors also influence the crack growth rate of solder joints. One such factor would be intermetallic formation which was omitted in the modeling study. Intermetallic particles form between plating materials and the solder joint, and evolve during accelerated testing, but the modeling tools lack the capability of capturing this phenomenon of intermetallic growth.

Conclusions

Reliability evaluation of GM test samples was conducted in two rounds of testing. The solder material in the first round of samples did not fail under accelerated tests within a reasonable amount of time and thus, a predictive lifetime model could not be formulated. A different sample geometry was used for the second round of testing. Under all accelerated tests, type 3 samples performed the worst. Type 1 samples performed slightly better than type 2 samples - but not by much. In the thermomechanical modeling study, strain energy density results were obtained for all sample type configurations under the various accelerated test profiles. A predictive lifetime model was developed by correlating the modeling results with experimentally obtained results from accelerated tests. The predictive model can be used to estimate the lifetime of similar sample packages under the same accelerated test conditions, and can help with the time- and cost-effective design of new power electronic modules.

Subject Inventions Listing:

None

Report Date:

11 July 2016

Responsible Technical Contact at Alliance/NREL:

Paul Paret

Name and Email Address of POC at Company:

Zilai Zhao, zilai.zhao@gm.com

This document contains NO confidential, protectable, or proprietary information.